

Chapter 3

Beyond Ising SK

m-vector, Potts, *p*-spin, spherical, induced moment, random graphs

David Sherrington

Rudolf Peierls Centre for Theoretical Physics, Oxford OX1 3PU, UK

Jairo R. L. de Almeida

*Departamento de Física, Universidade Federal de Pernambuco, Recife,
Brazil*

This chapter introduces a variety of spin glass models, beyond the simple Sherrington-Kirkpatrick (SK) version, that have led to enriched understanding and application.

3.1 Introduction

When one of us introduced the SK model [1], with Kirkpatrick in 1975, following the very innovative paper of Edwards and Anderson [2] earlier the same year, he made two choices that have proven to be influential; (i) an infinite-range intensive exchange distribution and (ii) Ising spins; the first in the hope of enabling an exact solution by analogy with and extension of previously known work on pure magnets and to provide the correct mean-field solution; the second to simplify the technicalities. In the event, the correct mean-field solution turned out to be much more subtle and interesting than was anticipated and thus revealing that mean-field theory need not be trivial – a common perspective at the time. The use of discrete Ising spins was serendipitous in highlighting a problem with a ‘natural’ (replica-symmetric) ansatz, recognized through an unphysical negative entropy feature already in SK. (The problem would not have been obvious

for continuous classical spins where such a feature is a known pathology¹.) The probable origin of the unphysical behaviour was later shown by the demonstration of an instability in an excitation mode in replica-space by the other of us and Thouless [3], eventually leading Parisi between 1979 [4] and 1983 [5] to the correct and highly impactful (full) replica symmetry breaking (RSB) resolution.

In this chapter we introduce systems with spins and interactions of different symmetries and indicate some of the qualitatively new consequences that arise. Mainly, we concentrate on systems with quenched infinite-range interactions, drawn randomly and independently from identical distributions, in conceptual analogy with SK, in the expectation of solvability in the thermodynamic limit $N \rightarrow \infty$ and the definition of the appropriate associated mean-field theories. We concentrate on equilibrium/Gibbsian statistical mechanics (statics), leaving dynamics to later chapters.

3.2 Binary interaction models

3.2.1 Local moment spins of $O(m)$ symmetry

In this section we consider systems with classical m -vector spins \mathbf{S}_i (m integral) beyond Ising ($m = 1$) and with SK-like scalar-product interactions.

In the absence of anisotropy these have the Hamiltonian

$$H = - \sum_{(ij)} J_{ij} \mathbf{S}_i \cdot \mathbf{S}_j, \quad (3.1)$$

with the J_{ij} drawn independently randomly and symmetrically ($J_{ij} = J_{ji}$) à la SK, from a Gaussian distribution of mean² J_0/N and variance J^2/N . The subsequent behaviour is essentially as for the $m = 1$ case (For RS analysis see [7] and [8]). In particular, if the spin length normalisation is chosen as $|\mathbf{S}| = \sqrt{m}$ the spin glass transition temperature (in units with Boltzmann's constant set to unity, $k_B = 1$) is $T = J$.

Something new arises when anisotropic terms are included.

First, consider the application of a uniform uni-directional magnetic field, in a direction denoted below by 1,

$$H = - \sum_{(ij)} J_{ij} \mathbf{S}_i \cdot \mathbf{S}_j - \sum_i h S_i^1. \quad (3.2)$$

¹EA [2] considered $m = 3$ spins, presumably because the stimulating experiments at the time involved Heisenberg spins.

²The inclusion of a finite positive mean, originally by Sherrington and Southern [6], aims to emulate the concentration-dependence of experimental spin glass systems.

In 1981, Gabay and Toulouse [9] pointed out that this system would now have a new transition to a spin glass phase transverse to the field direction (*i.e.* symmetric in the $m \neq 1$ hyper-plane) beneath a characteristic (GT) line in (h, T) , starting from $T = 1$ for $h = 0$ and with h_{GT} going asymptotically to ∞ as $T \rightarrow 0$. Replica symmetry breaks beneath this line, gradually and strongly in the transverse direction (as for an $(m-1)$ -dimensional spin glass) but also weakly in the 1-direction, until a cross-over to stronger RSB around an AT-like (h, T) line [10–12]; see Figs 3.1 and 3.2.

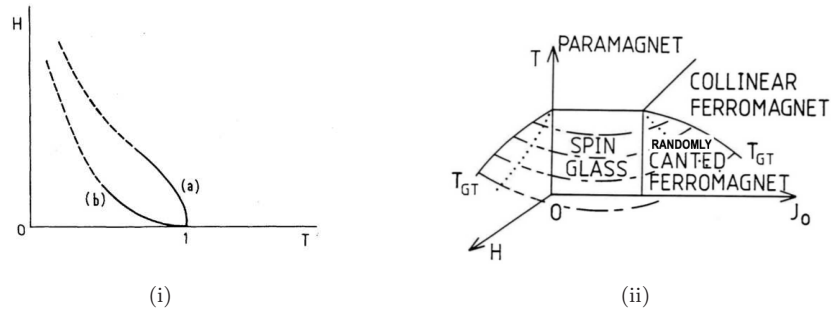


Fig. 3.1 m -vector phase diagrams: (i) $J_0 = 0$ in an applied field H : (a) GT transverse spin-glass line, (b) AT crossover (figure from [9], with permission. ©American Physical Society(1981), (ii) with also a positive exchange distribution mean J_0 ; solid lines denote phase transitions, dashed lines denote quasi-AT crossovers (figure adapted from [13], with permission ©Physical Society of Japan (1983)).

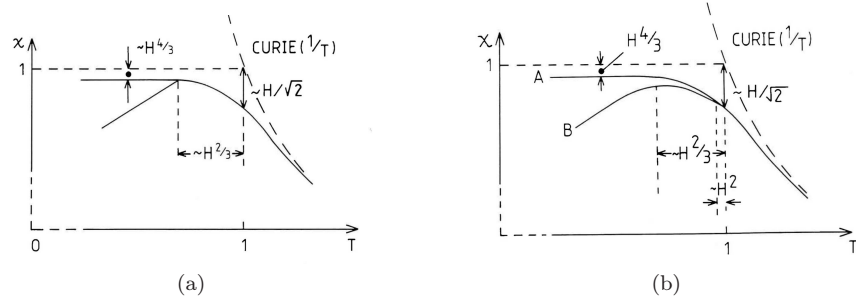


Fig. 3.2 Schematic longitudinal spin glass susceptibilities in field H : (a) Ising, (b) m -vector. The upper curves are field-cooled, the lower zero-field-cooled, reflecting the difference between $[1 - \int dx q_{||}(x)]/T$ and $[1 - q_{||max}]/T$. Figures from [13], with permission ©Physical Society of Japan(1983).

Second, for a $J_0 = 0$ $m > 2$ -vector system with external fields randomly and independently distributed over the full m -hypersphere there is no GT

analogue, only AT lines which are m -dependent [14]; see Fig.(3.3).

Third, consider the case with also quadratic single-site anisotropy

$$H = - \sum_{(ij)} J_{ij} \mathbf{S}_i \cdot \mathbf{S}_j - \sum_i h S_i^1 - \sum_i D (S_i^1)^2. \quad (3.3)$$

It exhibits three different spin glass phases already for $J_0 = 0, h = 0$, as shown in Fig.(3.4). All three phases exhibit full RSB. For a more general situation, including $J_0 \neq 0, h \neq 0$, RSB and Parisi solutions, see [15].

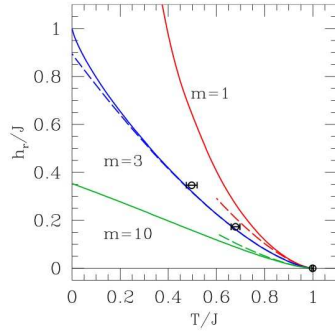


Fig. 3.3 AT line for m -vector spin glasses in quenched m -isotropic local random fields [14], with permission. ©American Physical Society (2010).

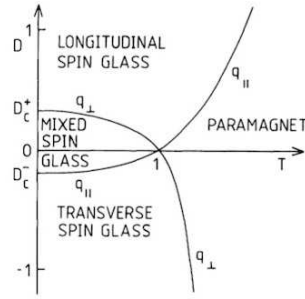


Fig. 3.4 Phase diagram of anisotropic spin glass. Figure from [16] ©IOP Publishing; see also [17].

3.2.2 Potts spins

All m -vector spins, including Ising ($m = 1$), have definiteness symmetry with pairwise interactions, J_{ij} and $-J_{ij}$ each leading to a unique relative ordering of the pair of spins i and j to minimize their energy. This is not the case for p -state Potts spins [18] with $p > 2$, where a ferromagnetic J prefers identical Potts states on i and j , whereas an antiferromagnetic J leads to $(p - 1)$ degenerate optima. To investigate possible consequences of the lack of this symmetry, Elderfield and Sherrington (1983) [19] considered the p -state Potts extension of SK³

$$H = \sum_{(ij)} J_{ij} (p \delta_{\pi(i)\pi(j)} - 1); \pi = 1, \dots, p \quad (3.4)$$

³Erzan and Lage [20] also introduced and studied the model, contemporaneously but independently.

where the J_{ij} are distributed as in eqn.(3.1).

This system turned out to have unusual RSB behaviour compared with the Ising higher m vector systems [19, 21, 22], as illustrated in Fig (3.5) for the Parisi order function $q(x); x \in (0, 1)$ for increasing p , based on formulae interpolated to real p .

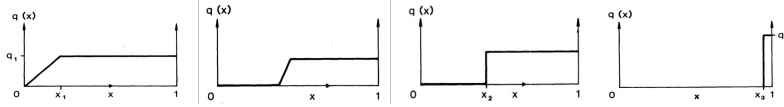


Fig. 3.5 Potts Glasses: Parisi order functions for small $\tau = (T_c - T)/T_c$;
(i) $p = 2 \equiv$ Ising (FRSB), (ii) $p_{c1} > p > 2$, (iii) $p_{c2} > p > p_{c1}$ (C1RSB),
(iv) $p > p_{c2}$ (D1RSB). Figures from [22]. ©Physical Society of Japan (1986)

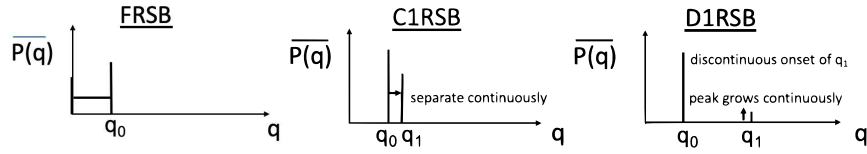


Fig. 3.6 Types of RSB $\overline{P(q)}$: (i) FRB ($p_{c1} > p > 2$); (ii) C1RSB (continuous onset) ($p_{c2} > p > p_{c1}$) (iii) D1RSB (discontinuous onset) ($p > p_{c2}$)

There are two critical Potts dimensions characterising significant changes in the overlap distribution; $p_{c1} = 2.82$ which separates a range of overlaps continuous between peaks at $q = 0$ and a finite q_{EA} , *i.e.* full RSB, and another with 1RSB, itself split into two parts, the first part on-setting continuously up to the second critical value $p_{c2} = 4$, the second part for $p > p_{c2}$, for which the 1RSB onset is discontinuous one-step [21] but without latent heat, now known as a ‘random first order transition’ (RFOT) [23] in recognition of the discontinuity in state-overlap as opposed to normal Ehrenfest first order; see Fig. (3.5). Corresponding overlap distributions, $\overline{P(q)}$, are illustrated in Fig (3.6).

Qualitatively similar behaviour is found in other systems lacking symmetry of definiteness; *e.g.* [24]

3.3 p -spin interactions

Another interesting and influential extension of the original binary-interaction SK model was introduced by Derrida in 1980 [25, 26], with the binary interaction term in the SK Hamiltonian replaced by one involving p

interacting spins.

3.3.1 Ising spins

Derrida considered p interacting Ising spins,

$$H_p = - \sum_{(i_1 i_2 \dots i_p)} J_{i_1 \dots i_p} \sigma_{i_1} \sigma_{i_2} \dots \sigma_{i_p}; \quad \sigma = \pm 1 \quad (3.5)$$

with the $J_{i_1 \dots i_p}$ randomly chosen from a Gaussian probability distribution of variance $J^2/N^{(p-1)}$. For $p \rightarrow \infty$ he showed that the problem simplifies into a random energy model (REM) which he solved exactly, demonstrating freezing into the lowest energy state below a critical temperature, corresponding to 1RSB but without the need for a replica formulation.

Subsequently, in 1984, Gross and Mézard [27] further considered the $p \rightarrow \infty$ model with several of the different methods used for the SK model – including the replica method – to explicitly exhibit the structure of the spin glass phase as 1RSB with a discontinuous transition.

In a further important study in 1985 [28], Gardner demonstrated for p -spin Ising systems that (i) for all $p > 2$ the spin glass transition from paramagnet to spin glass is 1RSB (whereas for $p=2$ (SK) the transition is full RSB (FRSB)) and (ii) that for $2 < p < \infty$ there is also a lower temperature (Gardner) transition to FRSB. Both observations have had further important ramifications, discussed in later chapters.

3.3.2 Spherical models

A solvable extension of the normal ferromagnetic Ising model, known as the *spherical model*, was introduced by [29], replacing the Ising variables $\sigma = \pm 1$ on each site $i = 1..N$ by a single (hyperspherical) condition $\sum_i^N \sigma_i^2 = N$, with the individual σ otherwise able to take any real value. A corresponding spherical extension of the (infinite-range $p = 2$) SK Ising spin glass model was introduced and solved by Kosterlitz et al. [30], shortly after SK, using several different mathematical procedures (including without needing replicas), and shown to exhibit a spin glass phase without replica symmetry breaking.

In a later study of the equilibrium statistical mechanics (statics) for the case of a spherical extension of the general- p -spin infinite-range (SK-extended) model, Crisant and Sommers (1992) showed that for $p > 2$ the spin glass state is 1RSB, with onset discontinuous below a critical magnetic field, continuous above it [31]. In a further (1993) paper on the relaxational

dynamics with Horner [32] they demonstrated several further intriguing features, including that the onset temperatures for 1RSB is higher for dynamics than that given by equilibrium statics. Later work recognised that the dynamical 1RSB onset corresponds to marginal stability of the statics.

Also in 1993, Cugliandolo and Kurchan [33] made a different study of the dynamics of the p -spin spherical model at long but finite times, demonstrating many unexpected but important new features, including ‘weak’ ergodicity breaking and aging effects, leading to much further activity and results, which will be expanded upon in later chapters.

Even though its statics do not exhibit RSB, the $p = 2$ spherical model was shown also to have non-trivial dynamics [34].

Fig. (3.7) shows examples of several models with various p -spin random zero-mean SK-extended interactions together with 2-spin ferromagnetic interactions, demonstrating several phases, including glassy ferromagnetism, and transitions.

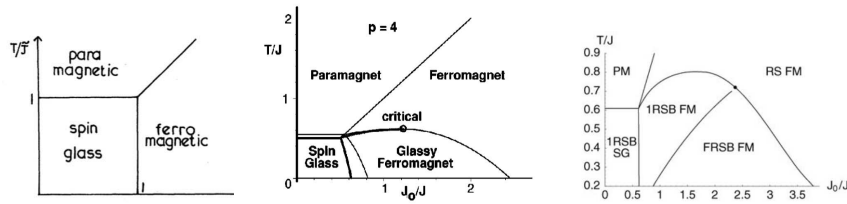


Fig. 3.7 Phase diagrams for p -spin random zero-mean interactions plus 2-spin ferromagnetic interactions: (i) spherical spins $p = 2$ (from [30] with permission. ©American Physical Society (1976)), statics, no RSB; (ii) spherical spins $p = 4$, statics (solid lines), dynamics (fine lines), dot (critical point, discontinuous 1RSB to left, continuous 1RSB to right.) (from [35] with permission. ©American Physical Society (1999)); (iii) Ising $p = 5$ statics, showing also 1RSB to FRSB transition (from [36] ©IOP Publishing (2001)).

There has also been significant interest in mixed- p spin glasses with infinite-ranged extended-SK interactions, particularly spherical models because of their solvability advantages along with realisation that they (mixed- p systems) can have FRSB as well as 1RSB, along with more complicated issues, both static and dynamic, of potential relevance to the understanding of other glasses; see *e.g.* [37–39] and later chapters in this book.

3.4 Finite-connectivity random graph models

Although the infinite-ranged SK model was introduced for its putative solvability rather than to mimic specific experimental systems, subsequent interest (and extension of the model) turned to many other problems where spatial separation is irrelevant, e.g., communication through the world wide web and random satisfiability in computer science. Several such problems are discussed in later chapters, but we here (briefly) discuss a few which appeared relatively early on in the field.

In 1985, Viana and Bray introduced a dimension-free but (on-average) finite-connectivity alternative to the SK spin glass model [38], in which active spins are effectively located on an Erdős-Renyi graph of average connectivity c with interactions on linked sites quench-randomly chosen from a distribution $P_c(J)$:

$$H = - \sum_{(ij)} J_{(ij)} \sigma_i \sigma_j; \quad P(J_{ij}) = (c/N)P_c(J_{ij}) + (1 - c/N)\delta(J_{ij}). \quad (3.6)$$

As for EA and SK, a spin glass phase results from sufficient frustration in $P_c(J)$, in purest form with $P_c(J) = P_c(-J)$, but without need for N -scaling of the mean or variance for c finite.

In 1986 Fu and Anderson [40] showed its relationship to graph bipartitioning⁴, including a demonstration of mapping the extensively connected graph problem to the SK model.

The Erdős-Renyi graph above has variable connectivity on different sites with only its average given by c . However, there is also much interest – particularly in computer science – in what are known as random *regular* graphs, where all vertices have same connectivity c , but still quench-disordered. This problem, with finite c , independent of the total number of vertices N , was considered numerically by Banavar *et al.* [41] in connection with optimal graph bi-partitioning, finding evidence for several of the novel features of the Parisi SK solution. The full analytical solution has proven harder than for SK, but RSB was found [42–44]. Further finite-connectivity random graph optimization studies, and extensions to classic computer science problems such as random satisfiability, have led to many new concepts, some of which will be discussed in later chapters.

⁴In the optimal graph bipartitioning problem one seeks a separation of vertices into two groups of equal size with the minimal number of graph edges between them. This problem is equivalent to finding the ground state of a system of Ising spins on the vertices of the graph interacting ferromagnetically along the edges but with a frustrating constraint of zero overall magnetization.

3.5 Induced moment spin glasses

Models considered thus far have moments (non-zero spins) even in the absence of interactions. For some systems, however, interactions are required to bootstrap-induce moments and exhibit cooperative magnetism. Ferromagnetic examples have been known for centuries and recognised for many decades, but here we make the case for spin glasses.

3.5.1 Discrete spins

Stimulated by consideration of local crystal field splitting favouring a singlet ground state, a discrete/‘hard’-spin example was introduced in 1977 by Ghatak and Sherrington (GS) [45], with Hamiltonian

$$H = -D \sum_i S_i^2 - \sum_{ij} J_{ij} S_i S_j; \quad S = 0, \pm 1, \quad (3.7)$$

with the J_{ij} Gaussian-distributed around zero mean. In the absence of the interaction term, for $D > 0$ the local term alone favours $S = \pm 1$, but for $D < 0$ it favours all $S = 0$, no moments. Consequently, for $D > 0$ the full system (including the interaction term) behaves qualitatively analogously to the SK model, while for $D < 0$ there is a critical maximum $|D|$ for interactions to induce bootstrap-induced cooperative order. At the RS level of description, the phase diagram is as shown in Fig.(3.8) and demonstrates both continuous and (Ehrenfest) first order phase transitions from paramagnet to spin glass, along with re-entrance/inverse-freezing from spin glass to paramagnet. Including RSB modifies the details of the first order transition line but retains its qualitative character [46].

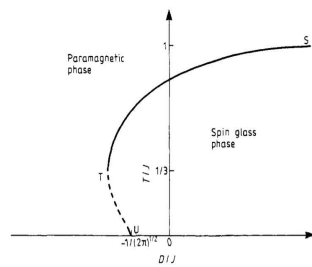


Fig. 3.8 Phase diagram of Ghatak-Sherrington model; figure from [47] ©IOP Publishing (1985) : The solid curve indicates a continuous transition between paramagnet and spin glass, the dashed curve a thermodynamically first order transition. The spin glass phase is full RSB.

3.5.2 Itinerant spin glasses

A simple ‘soft’-spin induced-moment spin glass model was initially proposed in 1973 by Sherrington and Mihill [48, 49], to try to explain the magnetic

behaviour of the transition-metal spin-glass alloy **RhCo**; see Fig(3.9) [50]⁵. Starting from a disordered Hubbard model alloy of ions with different Coulomb U , transforming to auxiliary local magnetization fields and with some simplification, including static approximation, leads to an effective Hamiltonian of the form

$$H = \sum_i \{ \kappa_i |\mathbf{m}_i|^2 + \lambda_i |\mathbf{m}_i|^4 \} - \sum_{(ij); i \neq j} J(\mathbf{R}_{ij}) \mathbf{m}_i \cdot \mathbf{m}_j, \quad (3.8)$$

where the i, j label sites, the \mathbf{m}_i are unconstrained local magnetization variables, the local coefficients κ_i and λ_i depend on the type of atom at site i , and the $J(\mathbf{R}_{ij})$ are inter-site interaction energies⁶.

$\kappa < 0$ would favour local moments (ground state with $m \neq 0$ in the absence of interactions), the analogue of $D > 0$ in the GS model; cf [51]. But for both Rh and Co the κ are positive, so that the local harmonic terms alone favour no moment, $|\mathbf{m}| = 0$. Inclusion of the interaction term, however, offers the potential for bootstrapped collective order if the resultant binding energy can overcome the local cost. For pure Co this results

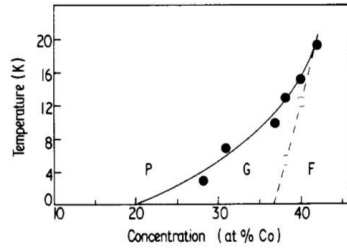


Fig. 3.9 **RhCo**; **P**aramagnet, **s**pin **G**lass, **F**erromagnet. Figure from [52] with permission. ©IOP Publishing (1975)

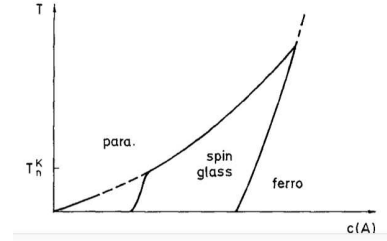


Fig. 3.10 Schematic prediction for **RhCo**-type alloy, from [48] with permission ©European Physical Journals.

in ferromagnetism, but the same is not true of Rh⁷ which consequently is

⁵Pure bulk Rh is non-magnetic, pure bulk Co is an itinerant ferromagnet, but isolated Co ions in Rh do not carry a long-lived moment and at very low concentrations of Co **RhCo** is Pauli paramagnetic. However, at intermediate concentrations a spin glass was observed, along with magnetic clustering features.

⁶In terms of the Hubbard model parameters, $\kappa_i = (1 - U_i \chi_{ii})$ and $J(\mathbf{R}_{ij}) = (U_i U_j \chi_{ij})$, where the U are the appropriate (site-occupation dependent) Hubbard potentials and χ_{ij} is the two-site conduction-band susceptibility.

⁷ $(1 - U_{Co} \sum_j \chi_{ij}) < 0$, $(1 - U_{Rh} \sum_j \chi_{ij}) > 0$.

not magnetic. Hence, already without need for computation, in analogies with local moment spin glasses (such as **Au** Fe) and itinerant ferromagnets (such as Ni), one can immediately anticipate a phase diagram with three low temperature phases as a function of increasing Co concentration of Pauli paramagnet, itinerant spin glass, and itinerant ferromagnet; see Fig(3.10)⁸.

3.5.3 Relaxor ferroelectrics as ‘soft’ pseudo-spin glasses

A similar reasoning provides a likely explanation for a long-standing puzzle in some displacive ferroelectric alloys and also opens up a potentially interesting new direction for random-field magnets.

Examples of pure displacive ferroelectrics are found in ionic crystalline compounds based on the generic formula ABO_3 with charges A^{2+} , B^{4+} , and O^{2-} , and at high temperature have cubic perovskite structure; see Fig (3.11). Inter-ionic interactions can lead to spontaneous structural distortions to lower symmetry at lower temperature if the consequential interaction energy lowering is great enough to overcome local displacement costs. With several ionic types within the unit cell, with different harmonic displacement coefficients, the displacements of the different ion types relative to their locations in the higher-temperature phase are themselves different, leading to spontaneous intra-cell electric dipole moments and hence ferro-electricity⁹. $BaTiO_3$ (BT) and $PbTiO_3$ (PT) are two classic examples and have been studied theoretically quantitatively using non-disordered and three-dimensional analogues of eqn.(3.8), with the local magnetizations replaced by displacements; *e.g* by [55,56]¹⁰; see again Fig (3.11).

The present interest, however, concerns substitutional alloys.

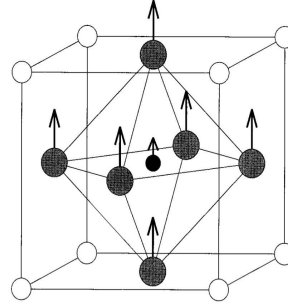
Already in the 1950s, experimental behaviour [57] retrospectively reminiscent of corresponding behaviour seen in the 1970s and 80s in experimental spin glasses [58,59] was observed in the alloy $Pb(Mg_{1/3}Nb_{2/3})O_3$ (PMN), with the Mg and Nb ions randomly distributed on the B-sites of

⁸Pre-EA, Sherrington and Mihil [48,49] were motivated by a desire to include statistically occurring local moment-like clustering. Post-EA, Hertz [53] examined a similar starting model, concentrating on prediction of an extended itinerant spin glass phase and proposed naming it *Stoner glass* in recognition of the pioneering work of Stoner [54] on itinerant (conduction electron) magnetism.

⁹Displacive ferroelectricity is thus an analogue of itinerant ferromagnetism.

¹⁰First-principles quantum-mechanical calculations are used to determine the parameters in effective classical Hamiltonians whose subsequent thermodynamical consequences are then explored through computer statistical mechanical simulations.

Fig. 3.11 ABO_3 perovskite. Circles show high T cubic cell: open circles = A, central black dot = B, dark shaded circles = O. Unit cell distorts to tetragonal ($c > a = b$) beneath T_c . Arrows show ionic displacements in the ferroelectric phase relative to the tetragonal cell. PbTiO_3 , from [56] with permission ©American Physical Society (1996).



the ABO_3 lattice, ; high, sharpish, strongly frequency-dependent peaks in AC susceptibility, see Figs. (3.12(i) and (ii)), but with no change in overall lattice structure and no ferroelectricity, again reminiscent of early spin glass experimentation that demonstrated spin freezing without periodicity. Other characteristic spin glass features, such as differences between FC and ZFC static susceptibilities beneath the static/low frequency susceptibility peak temperature, were observed later; see *e.g.* Fig. (3.13). Initially referred to simply as a *ferroelectric with diffuse phase transitions*, later the name *relaxor* was attributed to the new phase. Given their experimental similarity, theoretical comparison with spin glasses, with induced electric dipoles the analogues of local magnetizations, seems natural [60–63].

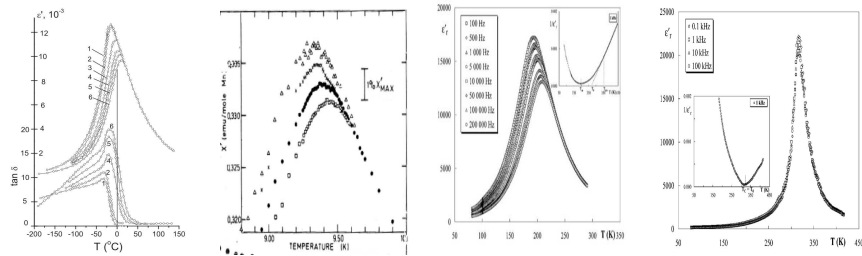


Fig. 3.12 AC susceptibilities: (i) heterovalent relaxor $\text{PbMg}_{1/3}\text{Nb}_{2/3}\text{O}_3$ (PMN), from [64] with permission ©Physical Society of Japan (1970); (ii) spin glass CuMn , from [59], with permission ©American Physical Society (1981); (iii) homovalent relaxor $\text{BaZr}_{0.35}\text{Ti}_{0.65}\text{O}_3$ (BZT), from [65], with permission ©IOP Publishing (2004); (iv) ferroelectric $\text{BaZr}_{0.20}\text{Ti}_{0.80}\text{O}_3$ from [65], with permission ©IOP Publishing (2004)

However, it is instructive to consider first the more recently discovered

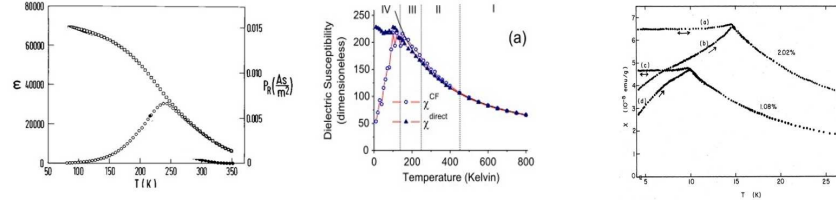


Fig. 3.13 Field cooled (FC) vs. zero-field cooled (ZFC) static susceptibilities; (i) PMN from [66], with permission ©American Physical Society (1998); (ii) BZT_{50/50} simulation, from [62], with permission ©American Physical Society;(2012) (iii) **CuMn** spin glass, from [67], with permission ©American Physical Society (1979).

alloy $\text{BaZr}_x\text{Ti}_{1-x}\text{O}_3$ (BZT) [65], in which the Ti and Zr B-ions are homovalent (both $4+$) and so without the extra, potentially complicating, charge- (and hence effective field-) disorder of PMN. The AC susceptibility for BZT with $x = 0.35$ is shown in Fig. (3.12(iii)). It looks very similar to those shown for PMN and **CuMn**, suggesting similar physics. (Again, the average crystal structure remains cubic perovskite and without global electric order.) The preparation-dependence of static susceptibilities also look similar, with a separation between field cooled and zero field cooled susceptibilities onsetting at the transition and growing as the temperature is reduced; see Fig (3.13).

Noting that pure BaZrO_3 is experimentally found not to exhibit ferroelectricity, in contrast to BaTiO_3 , one can already deduce that the local harmonic displacement coefficient of Zr^{4+} must be significantly greater than that of Ti^{4+} , too large for the interaction terms to overcome it^{11 12}.

The relaxor phase of BZT, as discussed above, is straightforwardly explainable by analogy with the induced-moment discussion above for a spin glass phase in **RhCo**, with Zr the analogue of Rh, Ti of Co, and the relaxor the analogue of a spin glass, with in-cell ionic displacements analogues of local magnetizations; see Figs. (3.5.3) and (3.5.3) Simulations of BZT_{50/50} using a model as discussed above have been performed by [62] (FC/ZFC; Fig (3.13)(ii)) and [68] (AC susceptibility), in good accord with experiments.

It is also interesting to compare the frequency-dependences of the location of the peaks in experimental AC susceptibility curves of $\text{BaZr}_x\text{Ti}_{1-x}\text{O}_3$

¹¹Note that, since Zr^{4+} and Ti^{4+} are homovalent, the strengths of the ionic Coulombic interactions in BT and BZ are essentially the same.

¹²In fact the coefficients can be calculated from numerical first-principles quantum mechanics. Another crude indicator comes from comparison of ionic radii.

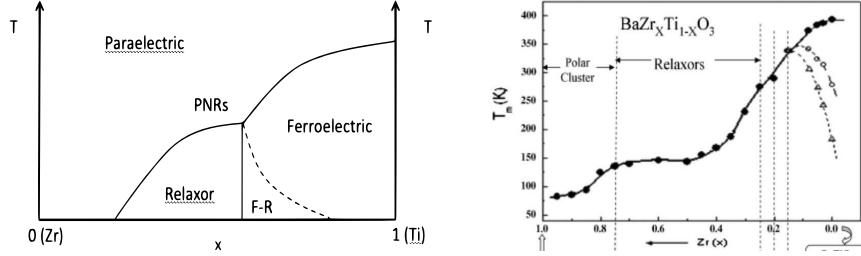


Fig. 3.14 **Left:** Heuristic phase diagram for BZT, by analogy with spin glass. PNRs refer to locally correlated statistical clusters (polar nano-regions) above the extended cooperative transition [63]. F-R refers to a possible mixed ferroelectric-relaxor. **Right:** Experimental phase diagram for BZT, from [69], with permission ©American Ceramics Society (2008)

for concentrations of the Zr ions above and below the critical concentration separating ferroelectric and relaxor. The ferroelectric transition peak temperature of the AC susceptibility for $x = 0.20$ (ferroelectric; Fig (3.12)(iv)) is essentially frequency-independent, as for a normal pure ferroelectric transition, while that for $x = 0.035$ (relaxor; Fig(3.12)(iii)) is highly frequency-dependent, as indeed are the peaks for spin-glass onset in low concentration **CuMn** (Fig(3.12)(ii)) and heterovalent relaxor PMN (Fig(3.12)(i)). It seems likely that the greater dispersion of the relaxors and spin glass, compared with their ferro counterparts, are consequences of the rugged and chaotically-evolving *free energy landscape* that underlies RSB.

Let us now return to the original, canonical and much studied relaxor PMN. It differs from BZT in that its site-occupation disorder is heterovalent, with the two types of B ions carrying different charges, Mg being 2+ and Nb 5+, rather than the 4+ of the normal pure (ABO_3) template. Being also randomly distributed, they effectively lead to extra quenched random fields in an extension of eqn.(3.8), in three dimensions.

Noting that Mg^{2+} has a similar ionic radius to Zr^{4+} and Nb^{5+} a similar ionic radius to Ti^{4+} , one can expect some B-ordering tendencies in PMN similar to those in BZT [70]. However, since $\text{PbZr}_x\text{Ti}_{1-x}\text{O}_3$ (PZT) has not been observed to exhibit relaxor behaviour, the random fields appear to be also necessary for the favouring of spin glass behaviour in PMN¹³

¹³An experimentally-based case for the important role of random fields in PMN was originally made by [71].

¹⁴. This further raises the issue of possible (quasi-)spin-glass behaviour in even-simpler systems with a combination of frustrated but non-random interactions and quenched local disorder only through random fields. Given that truly 3-dimensionally random local magnetic fields are impossible to produce experimentally, heterovalent relaxor alloys may provide fruitful alternative *experimental laboratories* for the study of their consequences.

A third feature observed experimentally in relaxors, and considered as one of their key characteristics, is of clusters of locally ordered regions above the (susceptibility-peak) transition temperature, generally referred to as ‘polar nano-regions’ (PNRs). Within the picture outlined above they are simply explainable for homovalent systems (such as BZT) as quench-statistically-occurring localized states in an analogue of Anderson localization [72] in which a ‘mobility edge’ determines the separation of cooperative extended order and insufficiently correlated PNRs, while a density-of-states ‘band edge’ emulates the limit of PNR observability [63, 73].

A minimal SK-analogue induced-moment model is

$$H = \sum_i (rm_i^2 + um_i^4) - \sum_{(ij)} J_{ij}m_i m_j, \quad (3.9)$$

[74], with the $\{J_{ij}\}$ drawn independently randomly from the infinite-ranged SK distribution, offering the possibility of exact solution¹⁵. However, since all the eigenstates of the SK-distribution for $\{J_{(ij)}\}$ are extended, no PNRs should result.

In summary, in this sub-section we have drawn attention to displacive relaxor ferroelectrics that display features that are reminiscent of spin glasses¹⁶. Although these features were observed already six decades ago and have led to considerable practical applications, their understanding nevertheless remains controversial. We have argued for an explanation as induced pseudo-spin glasses. Furthermore, by comparison of two different relaxor examples, homovalent and heterovalent, we speculate on an important role for quenched random fields in systems with spatially frustrated

¹⁴We might also note that Pb^{2+} is significantly more easily displaceable than Ba^{2+} ; in ferroelectric BT the relative displacements of Ba:Ti is 1:4 while in PT the relative displacements of Pb:Ti is 7:3, so that the undiluted A-site (Pb) ions play the dominant role in PMN, in contrast to the diluted B-site Ti-ions in BZT. This is in accord with the smaller ionic radius of Pb^{2+} compared with Ba^{2+} .

¹⁵It has also recently been proposed and studied in connection with low temperature vibrational excitations of structural glasses [75].

¹⁶For a discussion of pseudo-spin glass-like behaviour in material systems with pre-formed moments, see [76–78].

interactions, and on heterovalent relaxors as potentially valuable experimental ‘laboratories’ that do not exist for magnetic systems.

3.6 Short-range and lattice models

The discussions above have been principally in terms of range-free systems. Real experimental systems are normally lattice-based in physical dimensions, normally $d = 3$, sometimes with relatively short-ranged, but still frustrated, interactions (*e.g.* $\text{Eu}_x\text{Sr}_{1-x}\text{S}$), sometimes long-ranged but decaying with separation (*e.g.* AuFe , CuMn). There has been much theoretical investigation concerning whether such systems, particularly short-ranged, can have RSB, whether there is a lower critical dimension for an AT transition in a field and, if so, what. These issues will not however be further discussed here, but left to later chapters, as will many applications and extensions of concepts derived from infinite-ranged modelling.

3.7 Conclusion

We have introduced several extensions of the Ising SK spin glass model, to different kinds of variables/spins/pseudo-spins and several types of interactions, mostly still randomly drawn from range-free intensive distributions, indicating several of the new features that have been exposed by theorists’ ‘blue sky’ curiosity, mainly from the first few decades of spin glasses. We have also noted two examples of conceptual and technical transfers, to graph partitioning and relaxor ferroelectrics.

Later chapters will extend the developments and expose much further theoretical enlightenment and fruitful conceptual and practical progress in application to problems far beyond understanding the metallic alloys that stimulated the theory of spin glasses half a century ago.

Bibliography

- [1] D. Sherrington and S. Kirkpatrick, Solvable model of a spin glass, *Phys. Rev. Lett* **35**, pp. 1792–1796 (1975).
- [2] S. F. Edwards and P. W. Anderson, Theory of spin glasses, *J. Phys. F* **5**, pp. 965–974 (1975).
- [3] J. R. L. de Almeida and D. J. Thouless, Stability of the Sherrington-Kirkpatrick solution of a spin glass model, *J. Phys. A* **11**, pp. 983–990 (1978).
- [4] G. Parisi, Infinite number of order parameters for spin-glasses, *Phys.Rev.Lett.* **43**, pp. 1754–1756 (1979).
- [5] G. Parisi, Order parameter for spin-glasses, *Phys.Rev.Lett.* **50**, pp. 1946–1948 (1983).
- [6] D. Sherrington and B. Southern, Spin glass versus ferromagnet, *J.Phys.F* **5**, pp. L49–L53 (1975).
- [7] S. Kirkpatrick and D. Sherrington, Infinite-ranged models of spin glasses, *Phys. Rev. B* **17**, pp. 4384–4403 (1978).
- [8] J. R. L. de Almeida, R. C. Jones, J. M. Kosterlitz and D. J. Thouless, The infinite-ranged spin glass with m -component spins, *J. Phys. C* **11**, pp. L871–L875 (1978).
- [9] M. Gabay and G. Toulouse, Coexistence of spin-glass and ferromagnetic orderings, *Phys.Rev.Lett* **47**, pp. 201–203 (1981).
- [10] D. M. Cragg, D. Sherrington and M. Gabay, Instabilities of an m -vector spin glass in a field, *Phys. Rev. Lett* **49**, pp. 158–161 (1982).
- [11] D. Elderfield and D. Sherrington, Parisi solutions for the m -vector spin glass in a field”, *J. Phys. A* **15**, pp. L199–L203. (1982).
- [12] G. Toulouse, M. Gabay, T. C. Lubensky and J. Vannimenus, On the order of the spin glass transitions in mean field theory, *J.Physique.Lettres* **43**, pp. 109–113 (1982).
- [13] D. Sherrington, The infinite-ranged m -vector spin glass, in *Heidelberg Colloquium on Spin Glasses., Lecture Notes in Physics*, Vol. 192. Springer-Verlag, pp. 125–136 (1983).
- [14] A. Sharma and A. P. Young, de Almeida-Thouless line in vector spin glasses, *Phys. Rev. E* **81**, 061115 (2010).

- [15] D. Elderfield and D. Sherrington, Field and anisotropy effects in spin glasses: I. the collinear case, *J. Phys. C* **16**, pp. 4865–4888. (1983).
- [16] D. M. Cragg and D. Sherrington, Spin glass with local uniaxial anisotropy, *Phys.Rev.Lett* **49**, pp. 1190–1193 (1982).
- [17] S. A. Roberts and A. Bray, Phase-diagram for spin-glasses with uniaxial anisotropy, *J.Phys. C* **15**, pp. L527–L531 (1982).
- [18] F. Y. Wu, The Potts model, *Rev. Mod. Phys.* **54**, pp. 235–268 (1982).
- [19] D. Elderfield and D. Sherrington, The curious case of the Potts spin glass, *J. Phys. C* **16**, pp. L497–L503 (1983).
- [20] A. Erzan and E. J. S. . Lage, The infinite-ranged Potts spin glass model, *J. Phys. C* **16**, pp. L555–L560 (1983).
- [21] D. J. Gross, I. Kanter and H. Sompolinsky, Mean-field theory of the Potts glass, *Phys.Rev.Lett.* **47**, pp. 304–307 (1985).
- [22] D. Sherrington, Potts and related glasses, *Prog.Theor.Phys.Supp.* **87**, pp. 180–190 (1986).
- [23] T. R. Kirkpatrick, D. Thirumalai and P. Wolynes, Scaling concepts for the dynamics of viscous liquids near an ideal glassy state, *Phys. Rev. A* **40**, pp. 1045–1054 (1989).
- [24] P. M. Goldbart and D. Sherrington, Replica theory of the uniaxial quadrupolar glass, *J.Phys. C* **18**, pp. 1923–1940. (1985).
- [25] B. Derrida, Random-energy model: Limit of a family of disordered models, *Phys. Rev. Lett* **45**, pp. 79–82 (1980).
- [26] B. Derrida, Random-energy model: An exactly solvable model of disordered systems, *Phys. Rev. B* **24**, pp. 2613–2626 (1981).
- [27] D. J. Gross and M. Mézard, The simplest spin glass, *Nuc. Phys.* **B240**, pp. 431–452 (1984).
- [28] E. Gardner, Spin glasses with p -spin interactions, *Nuc. Phys.* **B257**, pp. 747–765 (1985).
- [29] T. H. Berlin and H. Kac, Spherical model of a ferromagnet, *Phys. Rev.* **86**, pp. 821–835 (1952).
- [30] J. M. Kosterlitz, D. J. Thouless and R. C. Jones, Spherical model of a spin-glass, *Phys. Rev. Lett.* **36**, pp. 1217–1220 (1976).
- [31] A. Crisanti and H.-J. Sommers, The spherical p -spin interaction spin-glass model: The statics, *Z.Phys.B* **87**, pp. 341–354 (1992).
- [32] A. Crisanti, H. Horner and H.-J. Sommers, The spherical p -spin interaction spin-glass model: The dynamics, *Z.Phys.B* **92**, pp. 257–271 (1993).
- [33] L. Cugliandolo and J. Kurchan, Analytical solution of the off-equilibrium dynamics of a long-range spin-glass model, *Phys.Rev.Lett* **71**, pp. 173–176 (1993).
- [34] L. Cugliandolo and D. Dean, Full dynamical solution for a spherical spin-glass model, *J.Phys. A* **28**, pp. 4213–4234 (1995).
- [35] J. A. Hertz, D. Sherrington and T. M. Nieuwenhuizen, Competition between glassiness and order in a multispin glass, *Phys.Rev. E* **60**, pp. R2460–R2463 (1999).
- [36] P. Gillin, D. Sherrington and H. Nishimori, Multispin ising spin glasses with ferromagnetic interactions, *J.Phys.A* **34**, p. 2949–2964 (2001).

- [37] A. Crisanti and L. Leuzzi, Spherical $2 + p$ spin-glass model: An exactly solvable model for glass to spin-glass transition, *Phys.Rev.Lett* **93**, 217203 (2004).
- [38] A. Crisanti and L. Leuzzi, Amorphous-amorphous transition and the two-step replica symmetry breaking phase, *Phys.Rev.B* **76**, 184417 (2007).
- [39] G. Folena, S. Franz and F. Ricci-Tersenghi, Rethinking mean-field glassy dynamics and its relation with the energy landscape: The surprising case of the spherical mixed p -spin model, *Phys.Rev.X* **10**, 031045 (2020).
- [40] Y. Fu and P. Anderson, Application of statistical mechanics to np-complete problems in combinatorial optimisation, *J.Phys.A* **19**, pp. 1605–1620 (1986).
- [41] J. R. Banavar, D. Sherrington and N. Sourlas, Graph bipartitioning and statistical mechanics, *J. Phys. A* **20**, pp. L1–L8 (1987).
- [42] K. Y. M. Wong and D. Sherrington, Intensively connected spin glasses: towards a replica-symmetry-breaking solution of the ground state, *J.Phys.A.* **21**, pp. L459–L466 (1988).
- [43] S. Franz, M. Leone, F. Ricci-Tersenghi and R. Zecchina, Exact solutions for diluted spin glasses and optimization problems, *Phys.Rev.Lett.* **87**, 127209 (2001).
- [44] M. Mézard and G. Parisi, The Bethe lattice spin glass revisited, *Eur.Phys.J. B* **20**, pp. 217–233 (2003).
- [45] S. K. Ghatak and D. Sherrington, Crystal field effects in a general S ising spin glass, *J.Phys. C* **10**, pp. 3149–3156 (1977).
- [46] A. Crisanti and L. Leuzzi, Thermodynamic properties of a full-replica-symmetry-breaking ising spin glass on lattice gas: the random Blume-Emery-Griffiths-Capel model, *Phys.Rev.B* **70**, 014409 (2004).
- [47] P. J. Mottishaw and D. Sherrington, Stability of a crystal-field split spin glass, *J.Phys. C* **18**, pp. 5201–5213 (1985).
- [48] D. Sherrington and K. Mihill, Effects of clustering on the magnetic properties of transition metal alloys, *J.Physique Supp.* **5 C4**, pp. 199–201 (1974a).
- [49] D. Sherrington and K. Mihill, Magnetic ordering in transition metal alloys, in *Proc. Int. Conf. Mag. (Moscow 1973)*, Vol. 1 (1). Nauka, Moscow, pp. 238–287 (1974b).
- [50] B. R. Coles, A. Tari and H. C. Jamieson, in *Low Temperature Physics LT13.*, Vol. II. Plenum, New York, pp. 414–418 (1974).
- [51] P. Anderson, Localized magnetic states in metals, *Phys.Rev.* **124**, pp. 41–53 (1961).
- [52] H. C. Jamieson, The approach to magnetic order in rhodium-cobalt alloys, *J.Phys.F* **5**, pp. 1021–1030 (1975).
- [53] J. A. Hertz, The Stoner glass, *Phys.Rev. B* **19**, pp. 4796–4804 (1979).
- [54] E. Stoner, Collective electron ferromagnetism, *Proc. Roy. Soc. A* **165**, pp. 372–414 (1938).
- [55] W. Zhong, D. Vanderbilt and K. M. Rabe, First-principles theory of ferroelectric phase transitions for perovskites: The case of BaTiO_3 , *Phys.Rev.B* **52**, pp. 6301–6312 (1995).
- [56] A. Garcia and D. Vanderbilt, First-principles study of stability and vibrational properties of tetragonal PbTiO_3 , *Phys.Rev.B* **54**, pp. 3817–3824

- (1996).
- [57] G. A. Smolenskii, V. Isupov, A. I. Agranovskaya and S. Popov, Сегнетоэлектрики с размытыми фазовыми переходами, *Fiz. Tverd. Tela* **2**, pp. 2906–2918 (1960), *Translation: Ferroelectrics with Diffuse Phase Transitions, Sov.Phys.Solid State* **2**, pp. 2594–2594 (1961).
 - [58] V. Cannella and J. Mydosh, Magnetic ordering in gold-iron alloys, *Phys.Rev. B* **6**, pp. 4220–4237 (1972).
 - [59] C. Mulder, A. van Duynveldt and J. Mydosh, Stability of a crystal-field split spin glass, *Phys.Rev. B* **23**, pp. 1384–1396 (1981).
 - [60] D. Viehland, M. Wuttig and L. E. Cross, The glassy behavior of relaxor ferroelectrics, *Ferroelectrics*. **120**, pp. 71–77 (1991).
 - [61] R. Pirc and R. Blinc, Spherical random-bond–random-field model of relaxor ferroelectrics, *Phys.Rev.B* **60**, pp. 13470–13478 (1994).
 - [62] A. R. Akbarzadeh, S. Prosandeev, E. J. Walter, A. Al-Barakaty and L. Bellaiche, Finite-temperature properties of Ba(Zr,Ti)O₃ relaxors from first principles, *Phys.Rev.Lett.* **108**, 257601 (2012).
 - [63] D. Sherrington, BZT: A soft pseudospin glass, *Phys.Rev. Lett.* **111**, 227601 (2014).
 - [64] G. A. Smolensky, Physical phenomena in ferroelectrics with diffused phase transition, *J.Phys.Soc.Jpn. Supp.* **28**, pp. 26–37 (1970).
 - [65] A. Simon, J. Ravez and M. Maglione, The crossover from a ferroelectric to a relaxor state in lead-free solid solutions, *J.Phys.Cond.Mat.* **16**, pp. 963–970 (2004).
 - [66] A. Levstik, Z. Kutnjak, C. c and R.Pirc, Glassy freezing in relaxor ferroelectric lead magnesium niobate, *Phys. Rev. B* **57**, pp. 11204–11211 (1998).
 - [67] S. Nagata, P. H. Keesom and H. R. Harrison, Low-dc-field susceptibility of CuMn spin glass, *Phys.Rev. B* **19**, pp. 1633–1638 (1979).
 - [68] D. Wang, A. Bokov, Z.-G. Ye, J. Hlinka and L. Bellaiche, Subterahertz dielectric relaxation in lead-free ba(zr,ti)o3 relaxor ferroelectricsl, *Nature Comm.* **7**, 11014 (2016).
 - [69] T. Maiti, R. Guo and A. S. Bhalla, Structure-property phase diagram of BaZr_xTi_{1-x}O₂, *J. Am. Ceram. Soc.* **91**, pp. 1769–1780 (2008).
 - [70] D. Sherrington, Pb(Mg_{1/3}Nb_{2/3})O₃: A minimal induced-moment soft pseudospin glass perspective, *Phys.Rev..B* **89**, 064105 (2014).
 - [71] V. Westphal, W. Kleemann and M. Glinchuk, Diffuse phase transitions and random-field-induced domain states of the relaxor ferroelectric PbMg_{1/3}Nb_{2/3}O₃, *Phys.Rev.Lett.* **68**, pp. 847–850 (1992).
 - [72] P. Anderson, Absence of diffusion in certain random lattices, *Phys.Rev.* **109**, pp. 1492–1505 (1958).
 - [73] D. Sherrington, What can spin glass theory and analogies tell us about ferroic glasses? in *Frustrated Materials and Ferroic Glasses, Springer Materials Science*, Vol. 275. Springer, pp. 1–29 (2018).
 - [74] D. Sherrington, Relaxors, spin, Stoner and cluster glasses, *Phase Transitions* **88**, pp. 202–221 (2015).
 - [75] E. Bouchbinder, E. Lerner, C. Rainone, P. Urbani and F. Zamponi, Low-frequency vibrational spectrum of mean-field disordered systems, *Phys. Rev.*

Bibliography

21

- B* **103**, 174202 (2021).
- [76] K. Binder and J. D. Reger, Theory of orientational glasses: models, concepts, simulations, *Adv.Phys.* **41**, pp. 547–627 (1992).
- [77] D. Sherrington, Understanding glassy phenomena in materials, in T. Kakeshita, T. Fukuda, A. Saxena and A. Planes (eds.), *Disorder and Strain induced complexity in functional materials*. Springer, pp. 177–199 (2012).
- [78] D. Sherrington, Materials physics and spin glasses, *J. Phys. A* **52**, 264001 (2019).